J. Fluid Mech. (1987), *vol.* 179, *pp.* 1–19
Printed in Great Britain

Characteristics of ejections in turbulent channel flow

By D. G. BOGARD† AND W. G. TIEDERMAN
School of Mechanical Engineering, Purdue University, W. Lafayette, IN 47907 USA

(Received 28 March 1986)

Quantitative measurements of the structure of ejections from the wall region have been made using conditional-sampling techniques. Discrete ejections from a burst event were identified using fluorescent-dye flow visualization simultaneously with streamwise, u, and normal, v, velocity measurements. These velocity measurements, at $y^+ = 15$, were conditionally sampled based on different phases of the ejection event. Features of the ejection which were educed from the conditional sampling were found to be very sensitive to the phase alignment. Results showed that ejections were characterized by a rapid deceleration at the leading edge followed by a strong positive velocity gradient at the trailing edge. An intense second-quadrant uv spike occurred immediately following the leading edge. This uv peak was highly correlated with a positive peak in the v velocity. The first ejection which occurred in a burst was found to be significantly more intense than the following ejections. Many characteristics of bursts which have been obtained from previous conditional-sampling studies were found to correspond to different phases of the ejection event.

1. Introduction

Conditional sampling has become an important technique for educing the general velocity characteristics of coherent structures in turbulent flows. There have been a large number of studies using this technique to investigate the structure in turbulent wall flows. The focus of many of these studies has been the burst or ejection which occurs in the near-wall region. One reason for the great interest in the burst event is the high uv Reynolds stress that has been associated with the event by the flow-visualization studies of Kim, Kline & Reynolds (1971) and Corino & Brodkey (1969). These studies indicated that most, if not all, of the second-quadrant uv (negative u and positive v) occurs during the burst event. Therefore, the burst is a very significant event in the production of turbulence.

Most of the previous studies using conditional sampling of the burst event have relied on identification of the burst using measured velocity data. A variety of different velocity characteristics have been postulated as being uniquely representative of the burst and used as a basis for burst detection. Many of these burst-detection algorithms have been evaluated by Bogard & Tiederman (1986) and the degree of effectiveness for each of the techniques in identifying bursts has been established. One major result of the Bogard & Tiederman study was that the velocity-based burst-detection algorithms are designed to detect discrete events which are more correctly associated with individual ejections within the burst rather

† Present address: Mechanical Engineering Department, University of Texas, Austin, TX 78712, USA

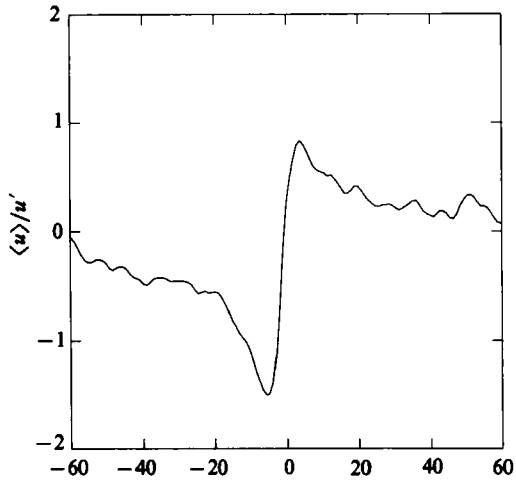

FIGURE 1. Ensemble-averaged u velocity using VITA conditional sampling. Average time $T^+ = 11$, $K = 1.0$, number of samples: 37.

than the total burst. Recall that a burst is the process of a streak breakup and may involve one or more ejections of streak filaments from the wall region (see Offen & Kline 1975; Bogard & Tiederman 1986).

At present, the most prominent technique used for burst or ejection detection is the variable-interval time-averaging (VITA) algorithm which was first used (for identifying bursts) by Blackwelder & Kaplan (1976). When used with a sufficiently high threshold, the ensemble average of conditional samples obtained with this technique has a very distinctive large, positive velocity gradient as shown in figure 1. The unique aspect of the VITA technique is that the characteristic large, positive velocity gradient does not occur when applying the technique to a random-noise signal. This result suggests that the VITA technique detects an event which is peculiar to turbulent wall flows, and this event has been generally assumed to be a burst. With the prominent use of the VITA technique by numerous researchers, the large, positive velocity gradient has become widely accepted as a characteristic of the burst event. However, Johansson & Alfredsson (1982) found that there are two distinct events detected with VITA – one group having a strong negative velocity gradient, and the other having a strong positive gradient. The strong positive gradient for the ensemble average of the conditional samples was found to be due to a greater number of positive-gradient events than negative-gradient events. The identification of these two distinctly different events raises the question of whether they should both be considered characteristic of an ejection.

Bursts have also been identified using the Quadrant technique which is based on the detection of the second-quadrant uv signal above a specified magnitude. Bogard & Tiederman (1986) showed that the Quadrant technique is the most effective detector of ejections. In contrast to the VITA results, conditional averages obtained by Alfredsson & Johansson (1984) using the Quadrant technique do not show an acceleration of the streamwise velocity to a value greater than the mean velocity. In a recent study using yet another burst-detection technique (based on strong activity in the high-frequency component of velocity) Rajagopalan & Antonia (1984) noted that the conditional average differed significantly from that obtained with the VITA technique.

One problem that is readily apparent for all conditional averages obtained with velocity-based detection algorithms, is that the conditionally-averaged signal always bears characteristics that can be directly related to the criteria used in the detection algorithm. For example, the VITA technique, although originally intended to measure periods of large variance in the velocity, is generally triggered by either a large positive or negative velocity gradient. The conditional average, as previously noted, reflects this characteristic. Similarly the Quadrant technique has a large negative uv spike in its conditional average, and the high-frequency velocity-component detection results in a conditional average that has a high-frequency oscillation. Consequently the significance of these conditional averages, especially in the sense of being representative of the characteristics of an ejection, is questionable.

A number of studies have been done that avoid reliance on velocity-based detection techniques by using temperature-contaminated fluid in the wall region. In studies by Chen & Blackwelder (1978) and Subramanian *et al.* (1982) the wall was heated very slightly so that fluid originating from the wall region could be detected by a measured temperature difference. Conditional averages were generated in these studies by detecting temperature fronts which had a sudden decrease in temperature and extended across the entire boundary layer. The resulting conditional average of the streamwise velocity displayed a strong positive gradient similar to the VITA results. However, it should be cautioned that this characteristic should be expected since a transition from hot to cold fluid would correspond to a transition from low- to high-velocity fluid since the hot fluid originates from the low-velocity wall region. Another difficulty with this technique is that no distinction can be made between ejections that are actively moving away from the wall and 'fossils' of ejections which occurred further upstream.

The ambiguity of the results obtained in previous conditional-sampling studies can be attributed to the uncertainty of how the detection technique is related to the burst. In the present study, the individual ejections within a burst were identified as distinct dye-marked elements of fluids actively moving away from the wall. Simultaneous velocity measurements were made with an X-type hot-film probe located at $y^+ = 15$. Conditional sampling of the velocity data was based on the flow-visualization records showing when an ejection was in contact with the probe. Furthermore, the stage of growth of the ejection, and its position with respect to the velocity probe, were taken into account when performing the conditional-sampling analysis.

When ensemble averaging conditionally sampled signals, the resulting signal patterns are very dependent on which part of the ejection is used to align each of the sampled signals. This is due to phase jitter or scrambling effects similar to those discussed by Blackwelder (1977) and Yule (1979) with respect to conditional samples taken at a point displaced from the detection point. In the present study the detection and conditional sampling are done at the same point but phase-scrambling effects still occur owing to the different sizes of the structures detected and because of the uncertainty of the precise time at which a particular part of the structure contacts the probe when using flow visualization for the detection. This phase scrambling was compensated for in two ways. First, specific parts of the structure were used as the detection or alignment point so that these parts were well phase aligned; hence, the characteristics of these individual parts of the structure were accurately represented. With this technique the overall characteristics of the structure are generally distorted due to phase scrambling of those parts of the structure distant from the detection point. In the other technique, compensation of the phase scrambling was done by non-dimensionalizing the timescale with respect to the size of the structure and more

accurate overall characteristics of the structure were obtained. This technique is similar to that used by Wallace, Brodkey & Eckelmann (1977) in the conditional sampling of TPAV-pattern-recognized signals. Since all of the structures have the same non-dimensionalized duration, each part of the structures is in phase alignment and the resulting ensemble-averaged signal pattern is representative of the general characteristics of the complete structure.

Results from this study are presented first in terms of the conditionally averaged signals of the streamwise velocity fluctuation, u, the normal velocity fluctuation, v, and the uv product in the four different uv quadrants. Following this, the ensemble average of conditional samples obtained by phase aligning with various parts of the ejection are presented. These results include effects due to the different stage of development of the ejection, and due to the position of the ejection within the total burst. Finally, results from the present investigation using flow visualization to identify ejections are compared to previous conditional sampling studies using velocity-based ejection-detection techniques. From these comparisons, the particular characteristics of the ejection upon which the various velocity-detection techniques tend to focus is evident.

2. Experimental procedures

Experiments were conducted in a recirculating, closed water channel using dye injection through a wall slot for flow visualization, and an X-type hot-film probe for velocity measurements. The equipment and procedures have been described in Bogard & Tiederman (1986) and Bogard (1982). Only a short description of the major facilities and techniques is presented here.

The channel had internal cross-sectional dimensions of 60×575 mm so that flow in the centre of the channel was two-dimensional. The length of the channel was 4.9 m with a dye slot spanning the bottom wall at 3.7 m. Tests were conducted in the region following the dye slot where the downstream distance was more than 60 channel heights ensuring fully-developed turbulent flow. A fluorescent dye was introduced into the channel through a 0.125 mm wide slot at a rate of $\frac{1}{20}$ the flow rate in the viscous sublayer ($y^+ < 8$). At this flow rate there was no appreciable disturbance to the flow and the dye accumulated in the low-speed sublayer streaks. A thin light-plane parallel with the flow and normal to the wall was used to illuminate the fluorescent dye. The light-plane width was less than 3 mm which was $w^+ = 22$ when normalized with inner variables. Since ejecting streak filaments typically span a distance of $l^+ = 100$ when moving away from the wall (see Bogard & Tiederman 1983), the light-plane only illuminated a relatively narrow section of the ejection. Recordings of the flow visualization were made with a high-speed video system (Video Logic Corporation Instar) at a framing rate of 120 f.p.s.

Velocity measurements in the water channel were made with a TSI model 1249-10W miniature hot-film X-probe. The two cylindrical sensors on the X-probe have diameters of 25 μm, lengths of 0.5 mm, and are separated by a distance of 0.5 mm. Normalized with inner variables the length and spacing of the sensors was $l^+ = 4$ which was sufficiently small to obtain accurate measurements of the turbulent structures (Blackwelder & Haritonidis 1983). Signals from the anemometers were digitized at a rate of 70 Hz per channel which corresponded to an interval between data points of $t^+ = 0.9$.

Experiments were performed in which simultaneous recordings were made of the

1. Ejection in the middle stage of development, clearly distinguishable and still strongly lifting (moving away from the near wall) as it passes through the probe (number of ejections: 37).
2. Later stage of development, clearly distinguishable and still lifting (but not strongly) at the probe (number of ejections: 49).
3. Early stage of development, ejections which originate very close to the probe but are not clearly distinguishable due to the short distance they can be viewed before they reach the probe (number of ejections: 32).
4. Ejection development has finished upstream of the probe with no apparent lifting when the probe is reached (number of ejections: 10).
5 Head of the ejection passes over the top of the probe with only the tail contacting the probe. The lifting or non-lifting of this tail is ambiguous (number of ejections: 17).
6. Head of the ejection passes over the top of the probe with the tail of the ejection clearly not lifting as it contacts the probe (number of ejections: 19).

TABLE 1. Ejection categories

dye flow visualization and the hot-film velocity measurements. The X-probe was located at $y^+ = 15$ above the lower wall of the channel and a distance $x^+ = 855$ downstream of the dye slot. At this position, the probe was in the centre of the 'full detection region' for ejections using dye-slot flow visualization. The 'full detection region' as shown by Bogard & Tiederman (1983), is a region downstream of the dye-slot where dye seeping through a wall slot marks all ejections.

The light-plane used to illuminate the fluorescent dye was aligned to pass directly through the X-probe. Since the segment of the ejection illuminated in the light-plane generally extended across the light-plane width, there was good correspondence between the measured velocities and the visualized ejections. Ejections were identified from a side view where the movement of the dye-marked streak elements moving away from the wall could be identified easily. A timing signal recorded with the flow visualization provided synchronization with recorded velocity signals.

Criteria for identifying ejections from flow-visualization records were the same as those used by Bogard & Tiederman (1986). Essentially the basic criterion was that there be definite outward movement of the streak filament from the wall region. The beginning of an ejection was identified as the point when the dye-marked filament passed above a level of $y^+ = 15$. For all ejections beginning at a distance greater than $x^+ = 200$ upstream of the probe, the dye-marked filament was required to display a movement of $\Delta y^+ \geqslant 20$ over a distance of $\Delta x^+ = 350$. For ejections beginning within $x^+ = 200$ of the probe a vertical movement of $\Delta y^+ \geqslant 10$ was required, and for those within $x^+ = 100$ a movement of $\Delta y^+ \geqslant 5$. Although arbitrary, these criteria were established to reduce the subjectivity of the flow-visualization analysis. For the most part the ejecting fluid elements displayed significantly greater vertical movement than the minimum requirements described above.

For each ejection, the following information was recorded: time of first contact with the probe, time contact ended, streamwise position of the origin, and ejection category. The ejection categories are described in table 1. The first four categories in this table classify the ejections in terms of the stage of development of the ejection when it contacts the probe. Categories 5 and 6 are ejections which for the most part pass above the probe and only a trailing tail from these ejections actually contacts the probe. These data were manually written into computer files. Conditional-sampling analysis of the velocity signal was then performed using the flow visualization as the basis for identifying ejections.

General statistics	Total sample time	200.6 s
	Number of ejections	164
	Average ejection period	0.389 s
	Intermittency of ejections	0.316
Conditional-averaged velocities		$\langle u\rangle/u' = -0.756$ $\langle v\rangle/v' = 0.300$ $\langle uv\rangle/\lvert\overline{uv}\rvert = -1.866$
Percentage uv contribution in each quadrant		$(uv)_1$: 16 % $(uv)_2$: 79 % $(uv)_3$: 62 % $(uv)_4$: 12 %

TABLE 2. Conditionally averaged velocities based on periods during which dye marked ejections were in contact with the probe

3. Results

The following results of conditional-sampling analysis are based on a continuous 200 seconds record of velocity and flow-visualization data. From analysis of the flow visualization 271 dye-marked events were identified of which 164 were classified as ejections. The number of ejections identified in each category is given in table 1. The total time during which an ejection was in contact with the probe was 63 seconds so that the average duration of an ejection was 0.389 seconds ($T^+ = 26$) and the intermittency of the ejections (ratio of the time the ejection is in contact with the probe to the total time) was 0.316. Results are presented first in terms of the conditionally-averaged signal levels, then the signal patterns obtained from the ensemble average of the conditional samples.

3.1. *Conditionally averaged signal levels*

For this analysis, velocity signals were averaged only for time periods during which flow visualization indicated an ejection was in contact with the probe. Results of the conditionally averaged u, v, and uv signals, normalized with the r.m.s. values u' and v' and the mean $\overline{uv}$ obtained from the full time record, are shown in table 2. Since an ejection involves the lifting of low-speed fluid, the conditionally averaged negative u and positive v signals are expected. The large value of the conditionally averaged uv shows that the ejection is an active producer of Reynolds stress.

More revealing data as to the importance of ejections in Reynolds-stress production comes from the analysis of the percentage of uv contribution in each quadrant during an ejection. Here the percentage $(uv)_i$ produced is defined as the integrated total of $(uv)_i$ during periods of ejections as compared to the integrated total for the total sample time. These results are also presented in table 2 and show large differences among the different quadrants. Since the intermittency of the ejections was 0.316, production of uv by a process uncorrelated to the ejections would result in a percentage contribution during ejections of approximately 32 %. As the results in table 2 show, production in each of the quadrants is either positively correlated (percentage contribution much larger than 32 %) or anti-correlated (percentage contribution much less than 32 %). The largest contribution is in quadrant 2 where 79 % of $(uv)_2$ was found to occur during ejections. This confirms that ejections are

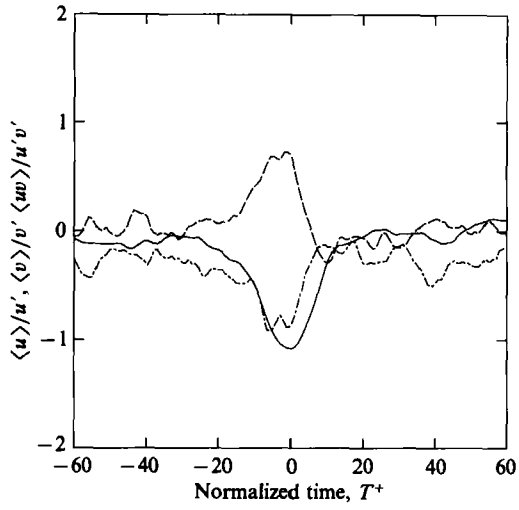

FIGURE 2. Ensemble-averaged velocities using visual conditional sampling, categories 1 to 5. Phase aligned with midpoint of dye contact. ——, $\langle u\rangle/u'$; – –, $\langle v\rangle/v'$; – – –, $\langle uv\rangle/u'v'$.

a major component in the production of negative Reynolds stress. Minimum contribution was found in $(uv)_4$, the other source of negative Reynolds stress. Since production of $(uv)_4$ is generally associated with sweep coherent structures (rushes of high-speed fluid towards the wall), a large contribution from this quadrant would not be expected during ejections. Contributions from the remaining two quadrants, $(uv)_1$ and $(uv)_3$, were also found to correlate with ejections. A 62% contribution of $(uv)_3$ indicates that this production is associated with the ejection process. The small 16% contribution of $(uv)_1$ indicates that the process responsible for production of this Reynolds stress does not occur during an ejection.

3.2. *Ensemble-averaged signal patterns phase aligned with visual cues*

Signal patterns characteristic of an ejection were obtained by ensemble averaging the velocity signals conditionally sampled at different phases of the ejection. Conditional samples were based on the 142 ejections in categories 1 to 5. Ejections from category 6 were not used in this analysis since only the tail of the ejections intersected the probe, and the tail of these ejections did not display an active lifting away from the wall.

The first ensemble average of conditionally sampled signals is shown in figure 2 where the samples are aligned with the centre of the ejections. The centre of the ejection was determined as the midpoint between the time the leading edge of the ejection first touched the probe and the time at which the trailing edge left the probe. Figure 2 shows basic characteristics of an ejection are a single negative u peak, a positive v peak, and a resulting negative uv peak. Dimensionless durations at the half-peak level for each of these are $T^+_{\frac{1}{2}}(u) = 17$, $T^+_{\frac{1}{2}}(v) = 14$, and $T^+_{\frac{1}{2}}(uv) = 14$. Peaks for v and uv occur slightly before $T^+ = 0$ at the centre of the ejection, but the u peak occurs at $T^+ = 0$.

When the leading edge and trailing edge of the ejection are used to phase align the conditional samples, the ensemble average of the signals are completely different as shown in figure 3. Different signal patterns occur with different phase alignments because ejections have widely different sizes. Because of this, only that part of the

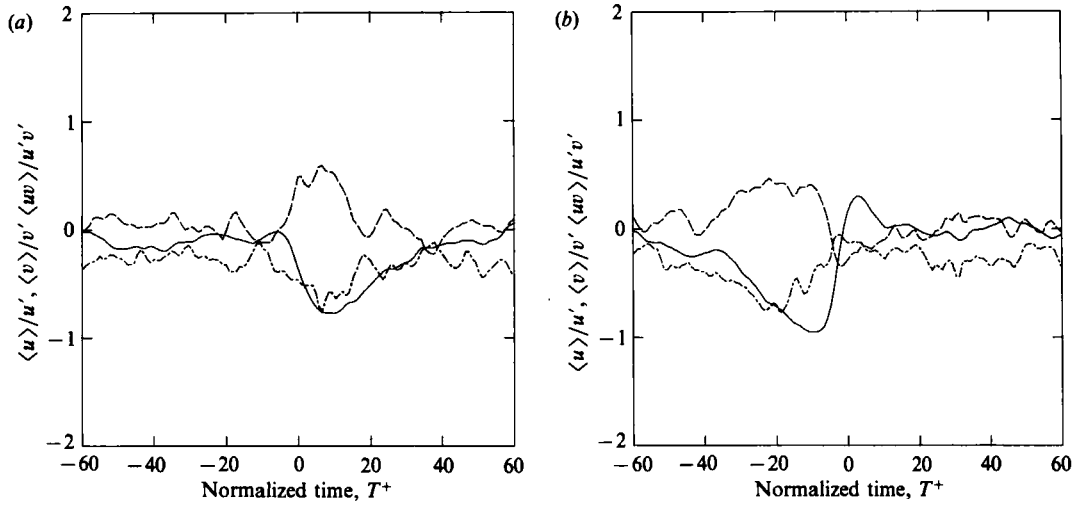

FIGURE 3. Ensemble-averaged velocities using visual conditional sampling, categories 1 to 5. Phase aligned with leading edge of dye contact (*a*) and trailing edge of dye contact (*b*). ——, $\langle u\rangle/u'$; – –, $\langle v\rangle/v'$; – – –, $\langle uv\rangle/u'v'$.

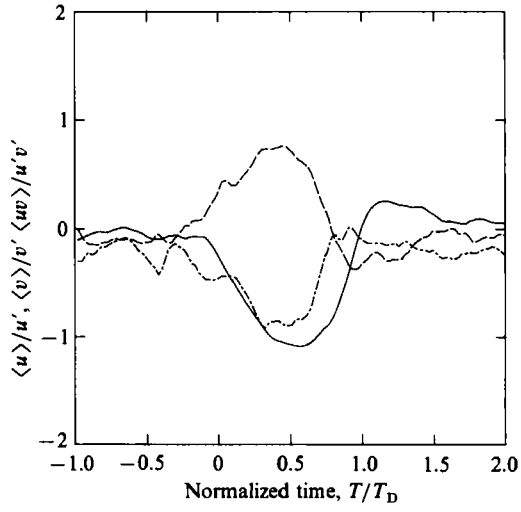

FIGURE 4. Ensemble-averaged velocities using visual conditional sampling, categories 1 to 5. Samples are normalized with the duration of dye contact, leading edge: $T/T_D = 0$ and trailing edge: $T/T_D = 1.0$. ——, $\langle u\rangle/u'$; – –, $\langle v\rangle/v'$; – – –, $\langle uv\rangle/u'v'$.

ejection in the immediate vicinity of the phase alignment point is a true characteristic of ejections. For example, alignment with the trailing edge of the ejection has a larger positive gradient and an overshoot to a positive u velocity which was not evident in the centre-aligned samples of figures 2.

The positive gradient in the u velocity at the trailing edge has a much larger magnitude than the negative gradient at the leading edge. However, both the v and uv peaks occur closer to the leading edge. Moreover the increased magnitude and decreased duration of these peaks indicate that the v and uv signals are in better phase alignment with respect to the leading edge.

To obtain a representation of the signal pattern for the complete ejection structure,

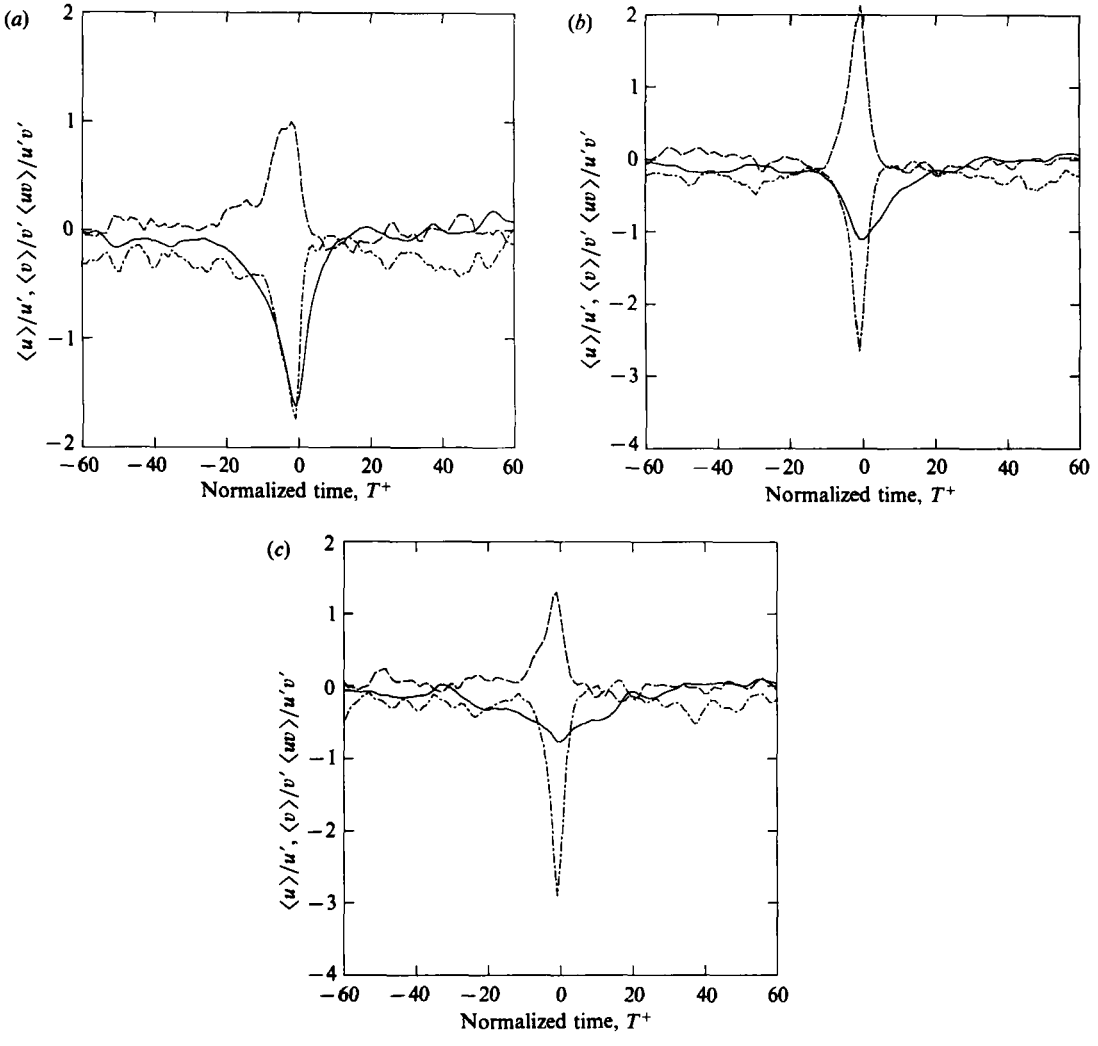

FIGURE 5. Ensemble-averaged velocities using visual conditional sampling, categories 1 to 5. Phase aligned with velocity characteristics occurring during the ejection: (*a*) maximum $-u$; (*b*) maximum v; (*c*) maximum $-uv$. ——, $\langle u\rangle/u'$; – –, $\langle v\rangle/v'$; – · –, $\langle uv\rangle/u'v'$.

the timescale for each ejection was normalized with respect to the duration of the ejection. The resulting signal patterns, figure 4, are essentially a composite of figures 2 and 3 since the normalized timescale ensures the simultaneous phase alignment of the leading edge, middle, and trailing edge. The general signal patterns shown in figure 4 are very similar to the centre-aligned samples of figure 2. However, in figure 4 the u velocity is shown to have a sudden change in slope at the leading edge rather than the gradual change as represented in figure 2. Also, immediately following the trailing edge the u velocity becomes positive which is a characteristic that was not apparent in figure 2.

3.3. *Ensemble-averaged signal patterns phase aligned with signal cues*

Since it was apparent that the general signal patterns of the ejections educed through conditional sampling was highly dependent on the phase alignment, further

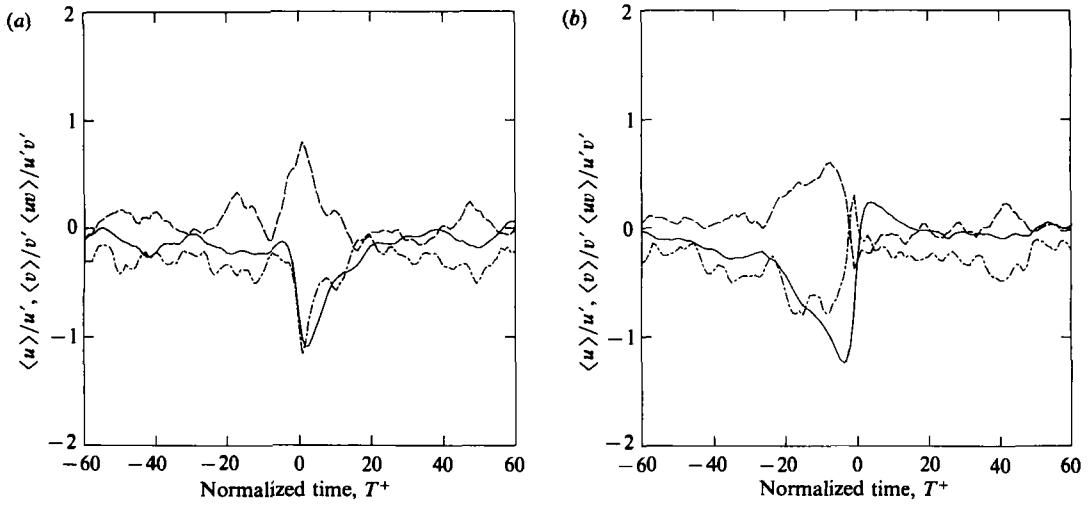

FIGURE 6. Ensemble-averaged velocities using visual conditional sampling, categories 1 to 5. Phase aligned with velocity characteristics occurring during the ejection: (*a*) maximum $-\mathrm{d}u/\mathrm{d}t$; (*b*) maximum $\mathrm{d}u/\mathrm{d}t$. ——, $\langle u\rangle/u'$; – –, $\langle v\rangle/v'$; – – –, $\langle uv\rangle/u'v'$.

conditional-sampling analysis was done using the velocity signals within the ejection for phase alignment. For this study, the time period for each ejection was searched for a specified velocity characteristic and samples were phase aligned with respect to this characteristic. Hence, the flow visualization of the ejections still provided the basis for selecting the conditional samples, but by using velocity characteristics to phase align the samples, a more precise representation of the general signal characteristics was obtained. This technique is similar to that suggested by Yule (1979) for phase shifting the individual patterns to obtain a 'phase-matched ensemble average'. The signal features used for this purpose were the peak levels of the $-u$, $+v$, and $-uv$ signals and the maximum positive and negative gradients of the u signal.

The resulting ensemble-averaged signal patterns for phase alignment with the $-u$, $+v$, and $-uv$ peaks, respectively, are shown in figure 5. It is immediately apparent from this phase alignment that the peak values of each of these velocity signals are much greater than was evident from phase alignment with visual cues. These results reveal that the signal peaks were not well phase matched in the previous alignments, which led to misleading representation of the true average peak levels. Also evident from the phase alignments in figure 5 is that the width of the peaks are significantly less than they appeared previously. Durations at the half-peak level are $T^+_{\frac{1}{2}}(u) = 13$, $T^+_{\frac{1}{2}}(v) = 5$, and $T^+_{\frac{1}{2}}(uv) = 4$.

The largest increase in peak levels was for the $-uv$ peak which increased by more than a factor 3 to a value $\langle uv\rangle = 3u'v'$. The magnitude of this peak is almost a factor 12 greater than the mean uv level making it a very distinctive feature of an ejection. Alignment with respect to the $-uv$ peak also results in a large increase in the v signal and the peaks for the two signals are coincident. Very similar characteristics were found from the alignment with respect to the $+v$ peak. These results show that the large $-uv$ spike is highly correlated with a similar $+v$ spike. When samples are aligned with the $-u$ peak, the $+v$ and $-uv$ peaks decrease substantially which indicates that the $-uv$ peak is not correlated as well with the u velocity as with the v velocity.

In figure 6 the conditional samples are phase aligned with respect to the maximum positive and negative u velocity gradients. This phase alignment was prompted by the results obtained from phase alignment with the leading and trailing edges of the ejections which were found to be associated with large negative and positive velocity gradients, respectively. Therefore, alignment with respect to the maximum u gradients can be viewed as a more precise phase alignment of the leading and trailing edges of the ejection.

The ensemble-averaged signal patterns in figure 6 are very similar to the leading- and trailing-edge patterns given in figure 2. Naturally the magnitude of the velocity gradients are increased in figure 6, and in both cases the duration of the event appears to be compressed. Also, from figure 6 it is readily apparent that the $+v$ and $-uv$ peaks are in better phase alignment with the leading edge (negative u gradient) of the ejection. With the better definition afforded by alignment with the positive u gradient at the trailing edge, a positive uv peak is educed from the conditional samples at the trailing edge. The narrow peak is apparently third quadrant uv due to a decrease in the v velocity to a negative value while the u velocity is still negative. The negative v velocity at the trailing edge was also evident in figure 2, but phase alignment was not good enough to show the positive uv peak.

3.4. *Signal patterns based on the stage of growth of ejections*

The conditional-sampling results presented so far have been based on all ejections in categories 1 to 5. Essentially these categories represent different stages of growth as the ejections come into contact with the probe. To determine how the signal characteristics change at different stages of growth, conditional samples were obtained using only ejections from specific categories. For example, characteristics of the early, middle, and late stage of growth of an ejection were represented by using ejections from categories 3, 1, and 2, respectively. The ensemble-averaged signal patterns based on samples of ejections in each of these categories are shown in figure 7. These conditional samples have been normalized with the ejection duration so that the ensemble-averaged signal patterns represent a composite with the leading edge, centre, and tailing edge in phase alignment. Conditional samples for categories 4, 5, and 6 are not presented since only a small number of samples were available for these categories.

Comparing the educed signal patterns at the different stages as shown in figure 7, the basic characteristics were found to be similar, and are comparable to the overall ejection characteristics given in figure 4. A large positive v velocity was found to occur at the leading edge of the ejection in the early stage. The magnitude of the v velocity at the leading edge fades for the later stages, but always remains positive. Both positive and negative gradients of the u velocity are relatively small in the early stage and the characteristic asymmetry of the u peak is not as evident at this stage.

All signal peaks are maximum at the middle stage of growth with the $-uv$ peak considerably larger than either the early or late stage. At the trailing edge of the ejection there is a third quadrant peak in the middle stage similar to that obtained in figure 6. However, this $(uv)_3$ peak is not evident in the early stage where the v velocity becomes negative immediately following the trailing edge. In the middle stage, the negative v velocity at the trailing edge has moved within the ejection where the u velocity is also negative; resulting in a positive quadrant 3 uv.

At the late stage of the ejection the $-uv$ and $+v$ peaks have decreased substantially, but the $-u$ peak has decreased only slightly from the maximum level. The

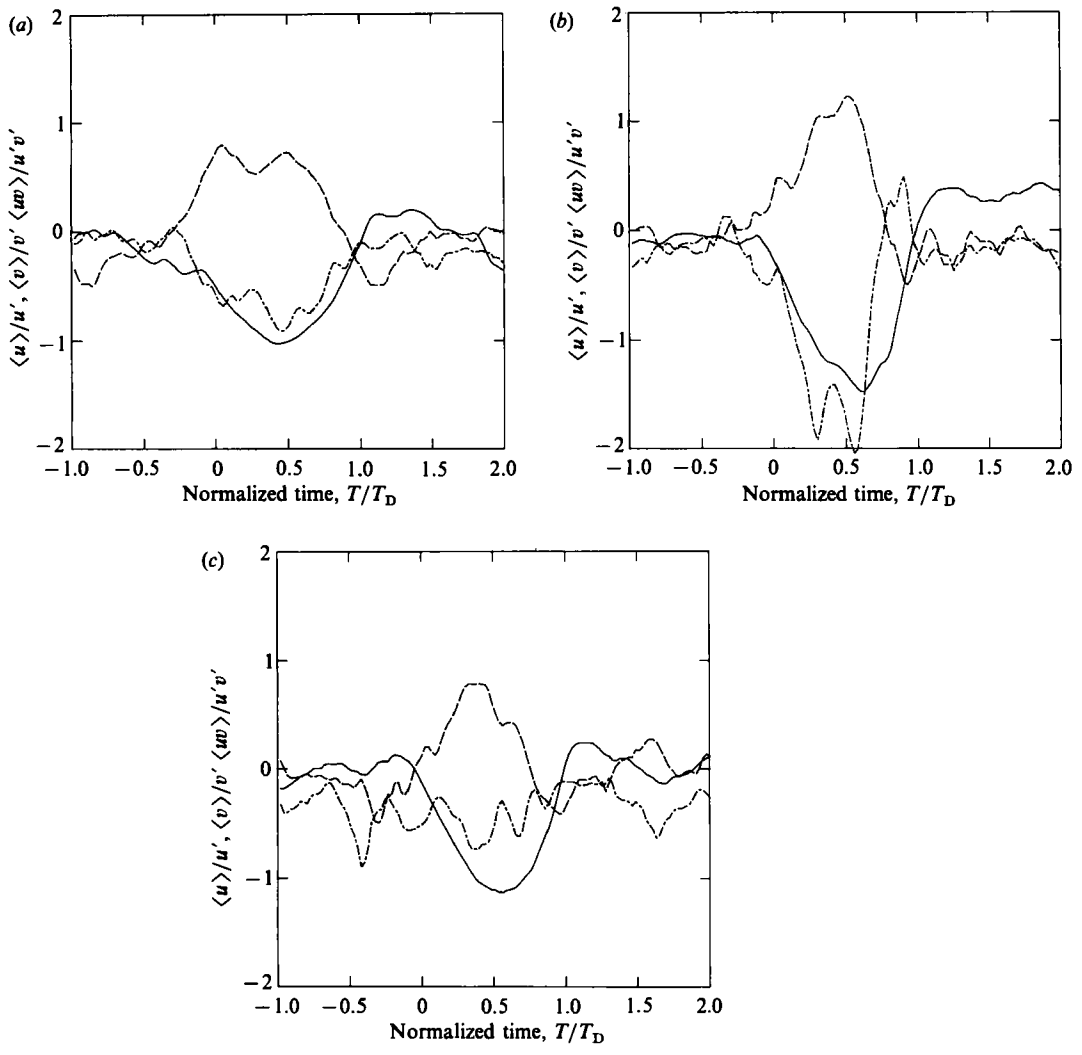

FIGURE 7. Ensemble-averaged velocities using visual conditional sampling. Samples based on the stage of growth: (*a*) category 2 – early stage; (*b*) category 1 – middle stage; (*c*) category 3 – late stage. All samples normalized with duration of dye contact. ——, $\langle u\rangle/u'$; – –, $\langle v\rangle/v'$; – · –, $\langle uv\rangle/u'v'$.

several peaks in the *uv* signal that appear in this conditional sample suggest that the *uv* signal is not well phase aligned.

3.5. *Signal patterns based on ejection position within a burst*

Frequently a closely spaced group of ejections form a burst; although some bursts have only a single ejection. Conditional sampling was performed to determine the differences in signal characteristics for ejections which occur in different positions of the burst. For this analysis, ejections were defined to be within the same burst if the period between ejections was less than $T_E = 0.8$ seconds ($T_E^+ = 53$). This definition was based on the criteria for determining the maximum time between ejections within the same burst as established by Bogard & Tiederman (1986). By this definition the 142 ejections in categories 1 to 5 were grouped into 86 bursts.

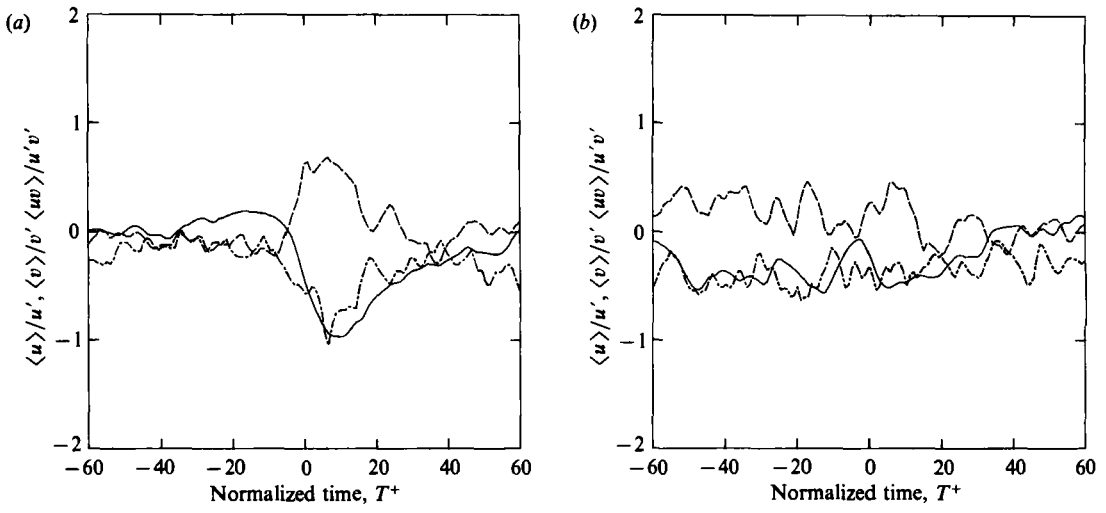

FIGURE 8. Ensemble-averaged velocities using visual conditional sampling, categories 1 to 5. Samples separated with respect to position within the burst; (*a*) first ejection (86 samples); (*b*) following ejections (57 samples). All samples phase aligned with leading edge. ——, $\langle u\rangle/u'$; – –, $\langle v\rangle/v'$; – – –, $\langle uv\rangle/u'v'$.

The conditional-sampling analysis was performed to determine how the leading edge of the first ejection in a burst differed from the following ejections, and how the trailing edge of the last ejection differed from the preceding ones. Results for the first ejection, and the following ejections phase aligned at the leading edge are given in figure 8. The conditional samples show a dramatic loss of coherence for ejections in a burst which follow the first ejection. In fact, peak levels in the u, v, and uv signals were found to be larger before the detection time for the leading edge of following ejections. Since the signals occurring before the detection time would be for the first ejection in a burst, but poorly phase aligned for these ejections, this result indicates that the ejections following the first ejection are much less intense than the first ejection. The domination of the first ejection in a burst is also reflected in the similarity of the ensembled-averaged signal patterns for the first ejection and the leading edge of all ejections shown in figure 3.

Conditional samples for the last ejection, and the preceding ejections were phase aligned with the trailing edge and these results are shown in figure 9. For both the last ejection and preceding ejections, the basic signal patterns are similar to the trailing-edge patterns for ejections given in figure 3. Note that many bursts have only a single ejection in which case the ejection would be classified both as the first ejection in a burst, and as the last ejection in a burst. Considering the results discussed previously for the first ejection in a burst, the relatively large $+v$ and $-uv$ peaks found for the last ejection in figure 9 were probably due to single ejection bursts. The relatively large $+v$ and $-uv$ peak levels for the ejections preceding the last ejection can also be attributed to the first ejection in a burst.

The conditional samples for the last ejection show a substantially greater positive gradient in the u velocity at the trailing edge than for the previous ejections. Unlike the conditional samples for the trailing edge of all ejections, figure 3, the u velocity was found to be slightly positive for a relatively long period following the last ejection. Also noticeable at the trailing edge of the last ejection is a large negative v velocity.

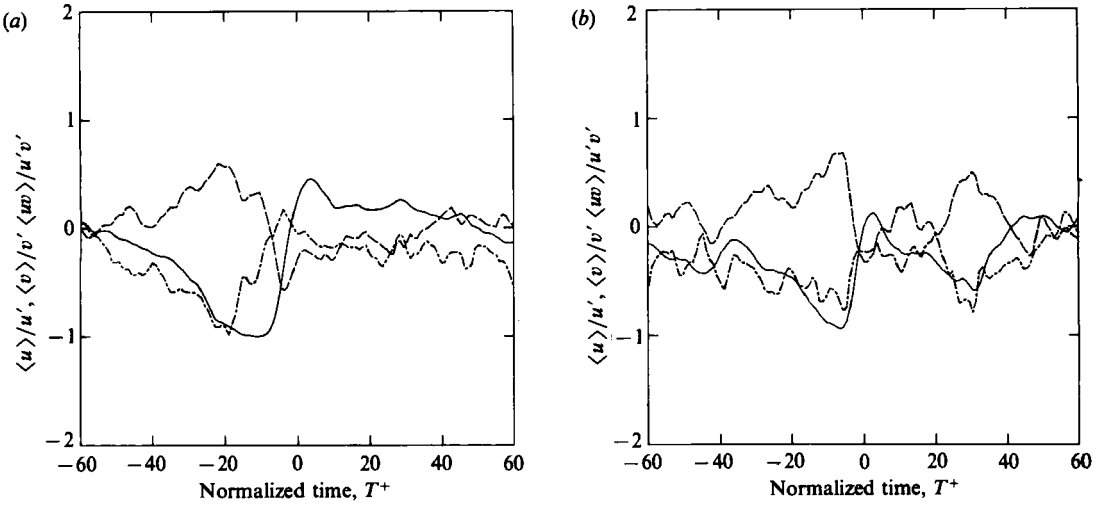

FIGURE 9. Ensemble-averaged velocities using visual conditional sampling, categories 1 to 5. Samples separated with respect to position within the burst; (*a*) last ejection (86 samples); (*b*) preceding ejections (56 samples). All samples phase aligned with trailing edge. ——, $\langle u\rangle u'$; – –, $\langle v\rangle/v'$; – – –, $\langle uv\rangle/u'v'$.

4. Discussion and comparison with previous conditional-sampling studies

To interpret the results of the conditional-sampling analysis it is useful to recall flow visualization of the ejection which shows that it is formed by the up-lifting of a low-speed streak element. When this low-speed fluid from the near-wall region rises into the higher-speed fluid above, the low-speed fluid will represent an obstacle onto which the high-speed fluid will impact and then flow around. The impingement of the high-speed fluid on the back of the low-speed element would cause a shear layer with a high velocity gradient. There would also be a shear layer at the front of the low-speed element, but the velocity gradient would not be as large here because there would not be a direct impingement of high-speed fluid. The conditional-sampling results are consistent with the above description of the ejection process in showing that the leading edge of the ejection has a negative velocity gradient which in general is smaller in magnitude than the positive gradient at the trailing edge.

The conditional-sampling analysis also revealed that, at the early stage, essentially all the streak fluid ejects away from the wall with the maximum vertical velocity at the leading edge. Large vertical velocities associated with the ejection result in a large second-quadrant uv being produced. As the ejections move away from the wall, high-speed fluid impinging on the trailing edge is moving towards the wall. Later in the growth of the ejection, low-speed fluid within the ejection is induced back towards the wall by the high-speed fluid impacting the back of the ejection. This interaction results in production of significant amounts of third-quadrant uv at the trailing edge.

Many of the conditionally sampled signal patterns obtained in this study were found to be similar to results found in previous investigations using velocity-based detection techniques. However, in the present study it was found that no single ensemble average of conditionally sampled signals fully describes the characteristics of an ejection. Moreover, the present results show how signal characteristics educed from previous studies are related to particular phases of the ejection.

Comparison of the present results with the conditional samples obtained with the VITA technique (figure 1), reveal that the VITA technique tends to educe the velocity characteristics of the trailing edge of the ejection. In the present study it was found that an ejection tends to have a stronger positive gradient at the trailing edge than the negative gradient at the leading edge. Consequently the VITA technique, which detects events with large velocity gradients, detects more positive gradient events from velocity measurements in the near-wall region. The large number of positive u velocity gradients results in an ensemble-averaged signal pattern with a large positive gradient characteristic of the trailing edge of an ejection.

When results for conditional samples aligned with the maximum positive velocity gradient, figure 6, were compared with the results obtained by Blackwelder & Kaplan (1976), similar trends were found for the u and v signals, but the uv signals were significantly different. In the present study only a single $-uv$ peak was found at approximately the centre of the ejection, whereas Blackwelder & Kaplan found two $-uv$ peaks occurring before and after the detection. This apparent discrepancy can be resolved by recognizing that the VITA technique will detect both positive and negative velocity gradients characteristic of the trailing and leading edges, respectively. Since the $-uv$ peak occurs after the leading edge, and before the trailing edge, the VITA technique detecting both the leading and trailing edges of the same ejection would place the same $-uv$ peak in two positions – before and after the detection time. This explanation is supported by the results of Alfredsson & Johansson (1984) who found that, when the VITA detections were resolved between detections of positive velocity gradients and negative gradients, only a single $-uv$ peak was educed from the conditional samples.

Comparing the peak levels obtained in the present study in figure 6 with those obtained by Blackwelder & Kaplan (1976), the present peak levels are significantly less. An explanation comes from the results of Bogard & Tiederman (1986) who showed that the VITA technique, with the threshold used by Blackwelder & Kaplan, only detected the large ejections. When comparing the Blackwelder & Kaplan results with ejections in the middle stage of growth, figure 7, the signal levels were found to be comparable.

Results obtained by Alfredsson & Johansson (1984), using VITA detections resolved into positive and negative slopes, would be expected to be comparable to the present results aligned with the trailing and leading edges, respectively. However, differences in the signal characteristics may exist because measurements by Alfredsson & Johansson were at $y^+ = 50$ while the present measurements were at $y^+ = 15$. Comparing the VITA detections with positive slopes to the present conditional samples aligned with the positive velocity gradient, figure 6, the signal patterns are similar although the VITA conditional samples show a more cohesive $-uv$ peak. Again signal levels for the VITA technique are larger because only major ejections are detected. A notable feature of the positive-slope VITA detections is a positive uv peak following the detection. This would appear to correspond to the third-quadrant uv peak identified in the present study at the trailing edge of the ejection.

Characteristics of the signals from the VITA detections with negative slope by Alfredsson & Johansson (1984) were very similar to the present conditional samples aligned with the negative slope, figure 6. The VITA signal levels were again larger due to the higher threshold used by Alfredsson & Johansson. Another noticeable feature was an improved phase alignment of the v and uv peaks with the negative slope VITA detections, similar to the improved alignment with the leading edge found in the present study.

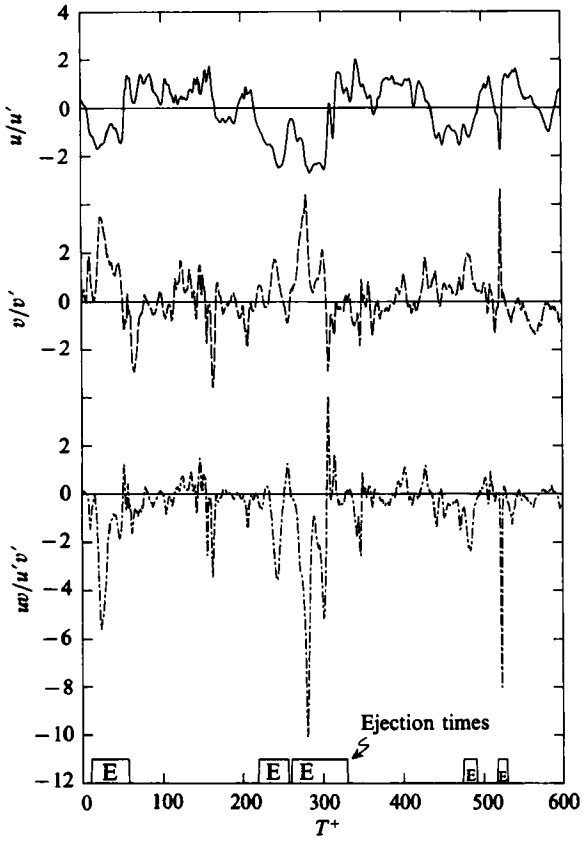

FIGURE 10. Typical real-time velocity signal with time periods marked during which flow visualization indicates an ejection in contact with the probe.

Conditional samples based on the detection of large $(uv)_2$ were obtained by both Comte-Bellot, Sabot & Saleh (1978) and Alfredsson & Johansson (1984). Comparisons with the results of Comte-Bellot *et al.* are somewhat tenuous since their measurements were made far from the wall ($y/R = 0.40$). Conditional samples by Comte-Bellot *et al.* were not aligned with the uv peaks, but rather with the point at which the $(uv)_2$ signal first passed a specified threshold. In effect this caused their conditional samples to be aligned with the negative slope of the uv signal. Consequently, the conditional samples for the v and uv peaks are highly asymmetric with larger gradients on the upstream sides. This contrasts with the symmetric signal peaks for v and uv found in the present study. These results emphasize the importance of phase alignment in conditionally sampled signal patterns.

Results from Alfredsson & Johansson (1984), at $y^+ = 50$, were aligned with the peak of the uv signal. The conditional samples for $(uv)_2$ detection show a stronger correlation of the $-uv$ peak to the $+v$ peak than the $-u$ peak, similar to the results in the present study. The widths at the half-peak levels were $T^+_{\frac{1}{2}}(v) = 4$ and $T^+_{\frac{1}{2}}(uv) = 3$. These compare to results in the present study, when aligned with the signal peaks, of $T^+_{\frac{1}{2}}(v) = 5$ and $T^+_{\frac{1}{2}}(uv) = 4$. Alfredsson & Johansson also found that the u peak was wider than the v and uv peaks.

The conditional-sampling study by Wallace *et al.* (1977) was based on detection of a signal pattern consisting of a deceleration of the u velocity followed by a stronger acceleration. Results from the present study show that this is in fact a characteristic

pattern of the ejection; however, it has not been proven to be a characteristic exclusive to ejections. Comparing the results obtained by Wallace *et al.* (1977) at $y^+ = 15$ to the present results normalized with the ejection duration, figure 4, the signal patterns were found to be very similar. Of particular interest were the similar characteristics found at the leading and trailing edges, represented in Wallace *et al.*'s data by negative and positive u velocity slopes respectively. Their conditional samples agreed with the present results in showing a positive v velocity at the leading edge, changing to a negative v velocity at the trailing edge, and a resulting positive uv peak at the trailing edge. However, the peak levels of the v and uv signals were $\frac{1}{3}$ of those for the present measurements while the u peak was $\frac{2}{3}$ of the present measurement.

As a final note, real-time velocity signals were examined in the light of the general characteristics of an ejection educed from the conditional-sampling analysis. Figure 10 shows a short-time history of the u, v, and uv signals, and the time periods during which flow visualization indicated an ejection was in contact with the probe. Immediately apparent is that the individual ejections do not have the relatively smooth signal patterns found in ensemble-averaged conditional samples. The difference between the two is due to random velocity fluctuations which often obliterate details in an individual ejection, but are smoothed out with conditional sampling. Despite this effect, examination of the real-time velocity data in figure 10 shows that the ejections are invariably associated with low u velocity, although often not with a single distinct peak. Also, the strong correlation with the $+v$ and $-uv$ peak is evident. A wide range of peak widths and amplitudes for the u, v, and uv signals is also apparent in figure 10. Consequently, the widths and amplitudes obtained in the conditional-sampling results should be regarded as average values.

5. Conclusions

The present measurements have confirmed that bursts are a key element in uv production in the near-wall region with approximately 80 % of $(uv)_2$ occurring during bursts. Moreover, uv in all four quadrants was found to be either correlated or anti-correlated with bursts. Higher levels of $(uv)_3$ and lower levels of $(uv)_1$ and $(uv)_4$ were found to occur during bursts than would be expected on a random basis.

A major finding of the conditional-sampling study was that the characteristics of the ensemble-averaged signals were highly dependent upon the phase alignment of the conditional samples. Even for the relatively short duration of the ejection event, phase scrambling causes significant loss in coherence for those parts of the ejection away from the phase-alignment point. Consequently, a combination of different phase alignments was required to educe the complete ejection structure.

An ejection was found to have the following generic velocity-signal characteristics:

a low-speed fluid element showing a sharp deceleration at the leading edge and a positive velocity gradient at the trailing edge. The magnitude of the velocity gradient at the trailing edge is generally greater than that at the leading edge;

on average the minimum u velocity is approximately $-2u'$ below the mean;

a narrow positive peak in the v signal which tends to occur immediately following the leading edge and on average is greater than $2v'$ in magnitude;

a narrow negative uv peak which on average is greater than $3u'v'$ in magnitude. This $-uv$ spike is a very distinctive characteristic of the ejection and is strongly correlated with the $+v$ peak;

at the trailing edge, in the later stage of development, low-speed fluid is induced back towards the wall resulting in significant $(uv)_3$ signal.

These characteristics were common to ejections at different stages of development, except the $(uv)_3$ peak at the trailing edge which was clearly evident only for ejections in the middle stage of growth. Also the first ejection within a burst was clearly stronger, i.e. more distinctive and larger amplitudes for the u, v, and uv signals, than the following ejections within the burst.

One of the more illuminating results from this study was that the many different signal characteristics of a burst educed by previous conditional-sampling studies are not contradictory, but are actually due to phase alignment with different parts of the ejection. VITA conditional samples tend to identify regions of large velocity gradients, with the positive and negative gradients corresponding to the trailing and leading edges of the ejection, respectively. On the other hand, the Quadrant technique which keys on the large $(uv)_2$ peak associated with an ejection, does not show the large u velocity gradients characteristic of the leading and trailing edges since its phase alignment is towards the centre of the ejection. Note also that previous conditional-sampling studies associated the signal patterns with a burst, when in fact the signals are characteristics of a single ejection within a burst.

The authors gratefully acknowledge Mr David T. Walker for his help in generating some of the plots used in this paper.

REFERENCES

ALFREDSSON, P. H. & JOHANSSON, A. Y. 1984 On the detection of turbulence-generating events. *J. Fluid Mech.* **139**, 325.

BLACKWELDER, R. F. 1977 On the role of phase information in conditional sampling. *Phys. Fluids* **20**, S232.

BLACKWELDER, R. F. & HARITONIDIS, J. H. 1983 Scaling on the bursting frequency in turbulent boundary layers. *J. Fluid Mech.* **132**, 87.

BLACKWELDER, R. F. & KAPLAN, R. E. 1976 On the bursting phenomenon near the wall in bounded turbulent shear flows. *J. Fluid Mech.* **76**, 89.

BOGARD, D. G. 1982 Investigation of burst structures in turbulent channel flows through simultaneous flow visualization and velocity measurements. Ph.D. thesis, Purdue University.

BOGARD, D. G. & TIEDERMAN, W. G. 1983 Investigation of flow visualization techniques for detecting turbulent bursts. *Symposium on Turbulence 1981*, p. 289. University of Missouri-Rolla.

BOGARD, D. G. & TIEDERMAN, W. G. 1986 Burst detection with single point velocity measurements. *J. Fluid Mech.* **162**, 389.

CHEN, C. P. & BLACKWELDER, R. F. 1978 The large-scale motion in a turbulent boundary layer; a study using temperature contamination. *J. Fluid Mech.* **89**, 1.

COMTE-BELLOT, G., SABOT, J. & SALEH, I. 1978 Detection of intermittent events maintaining Reynolds stress. In *Proc. Dynamic Flow Conf.-Dynamic Measurements in Unsteady Flows*, p. 213. Marseille, Baltimore, Skovlunde, Denmark.

CORINO, E. R. & BRODKEY, R. S. 1969 A visual study of turbulent shear flow. *J. Fluid Mech.* **37**, 1.

JOHANSSON, A. Y. & ALFREDSSON, P. H. 1982 On the structure of turbulent channel flow. *J. Fluid Mech.* **122**, 295.

KIM, H. T., KLINE, S. J. & REYNOLDS, W. C. 1971 The production of turbulence near a smooth wall in a turbulent boundary layer. *J. Fluid Mech.* **50**, 133.

OFFEN, G. R. & KLINE, S. J. 1975 A comparison and analysis of detection methods for the measurement of production in a boundary layer. In *Proc. 3rd Biennial Symposium of Turbulence in Liquids*, p. 289, University of Missouri-Rolla.

RAJAGOPALAN, S. & ANTONIA, R. A. 1984 Conditional averages associated with the fine structure in a turbulent boundary layer. *Phys. Fluids* **27**, 1966.

SUBRAMANIAN, C. S., RAJAGOPALAN, S., ANTONIA, R. A. & CHAMBERS, A. J. 1982 Comparison of conditional sampling and averaging techniques in a turbulent boundary layer. *J. Fluid Mech.* **123**, 335.

YULE, A. J. 1979 Phase scrambling effects and turbulence data analysis. *2nd Symp. on Turbulent Shear Flow*, p. 7–1. Imperial College, London.

WALLACE, J. M., BRODKEY, R. S. & ECKELMANN, H. 1977 Pattern-recognized structures in bounded turbulent shear flows. *J. Fluid Mech.* **142**, 121.